

Supporting Information

Energy Landscapes on Polymerized Liquid Crystal Interfaces

*Rachel S. Hendley,[†] Eugenie Jumai'an,[†] and Michael A. Bevan**

Chemical & Biomolecular Engineering, Johns Hopkins University, Baltimore, MD 21218

*Hector A. Fuster,[†] Nicholas L. Abbott**

Smith School of Chemical and Biomolecular Engineering, Cornell University, Ithaca, NY 14853

[†]These authors contributed equally to this work.

*To whom correspondence should be addressed: mavevan@jhu.edu, nla34@cornell.edu

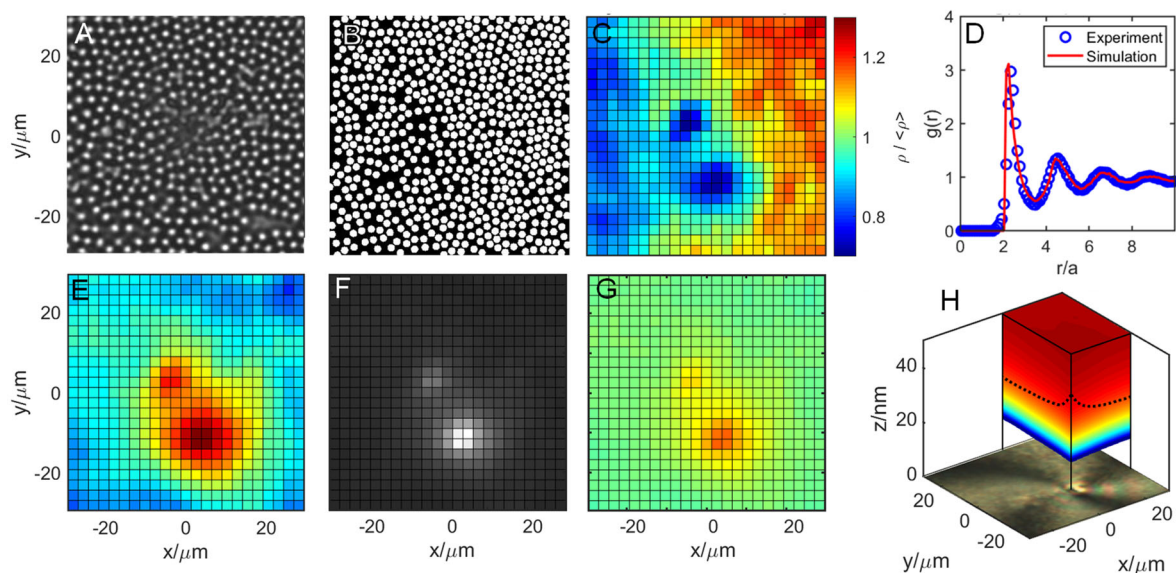


Fig. S1. Summary of diffusing colloidal probe experimental results, inverse MC simulations, and analysis of PLC defect in Fig. 5A (and Figs. 1-4). Representative configurations from (A) optical microscopy image of particles on PLC defect, and (B) rendering from converged equilibrated inverse MC simulation. (C) Experimental density profile over defect. (D) Pair correlation function from experiment (blue circles) and MC simulation (red line). (E) Converged interfacial energy landscape determined from inverse MC simulation ($\mu(x,y)=-6-0kT$, blue-red). (F) Position dependent brush thickness, ($2L_0(x,y)=25-35\text{nm}$, black-white). (G) van der Waals landscape evaluated at the onset of macromolecular repulsion ($\mu_V(x,y)=-4-0kT$, red-blue). (H) Optical characterization image and energy landscape quadrant cross sectional view centered on the defect with a dashed line showing the brush layer thickness at $h=2L_0$. Panels A-D are reported prior to removing the effect of surface tilt, whereas panel E-H show energy landscapes after removing the effect of a surface tilt ($\sim 150\text{ nm}$ over $\sim 50\ \mu\text{m}$) on the gravitational contribution.

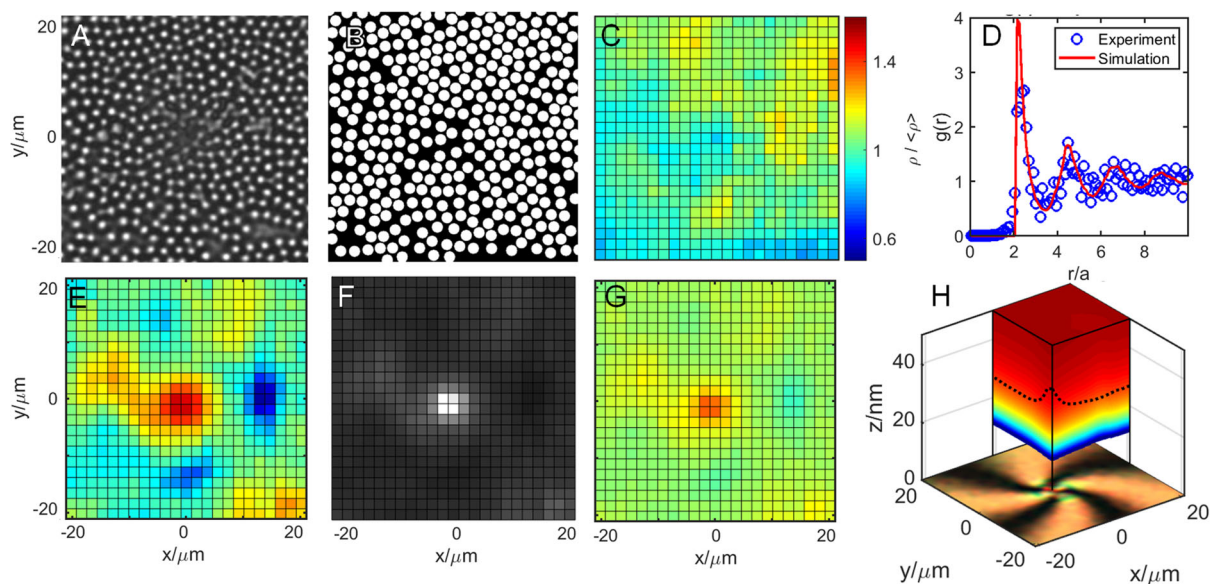


Fig. S2. Summary of diffusing colloidal probe experimental results, inverse MC simulations, and analysis of PLC defect in Fig. 5B. Representative configurations from (A) optical microscopy image of particles on PLC defect, and (B) rendering from converged equilibrated inverse MC simulation. (C) Experimental density profile over defect. (D) Pair correlation function from experiment (blue circles) and MC simulation (red line). (E) Converged interfacial energy landscape determined from inverse MC simulation ($u(x,y)=-6-0kT$, blue-red). (F) Position dependent brush thickness, ($2L_0(x,y)=25-35nm$, black-white). (G) van der Waals landscape evaluated at the onset of macromolecular repulsion ($u_V(x,y)=-4-0kT$, red-blue). (H) Optical characterization image and energy landscape quadrant cross sectional view centered on the defect with a dashed line showing the brush layer thickness at $h=2L_0$. Panels A-D are reported prior to removing the effect of surface tilt, whereas panel E-H show energy landscapes after removing the effect of a surface tilt (~ 450 nm over ~ 50 μm) on the gravitational contribution.

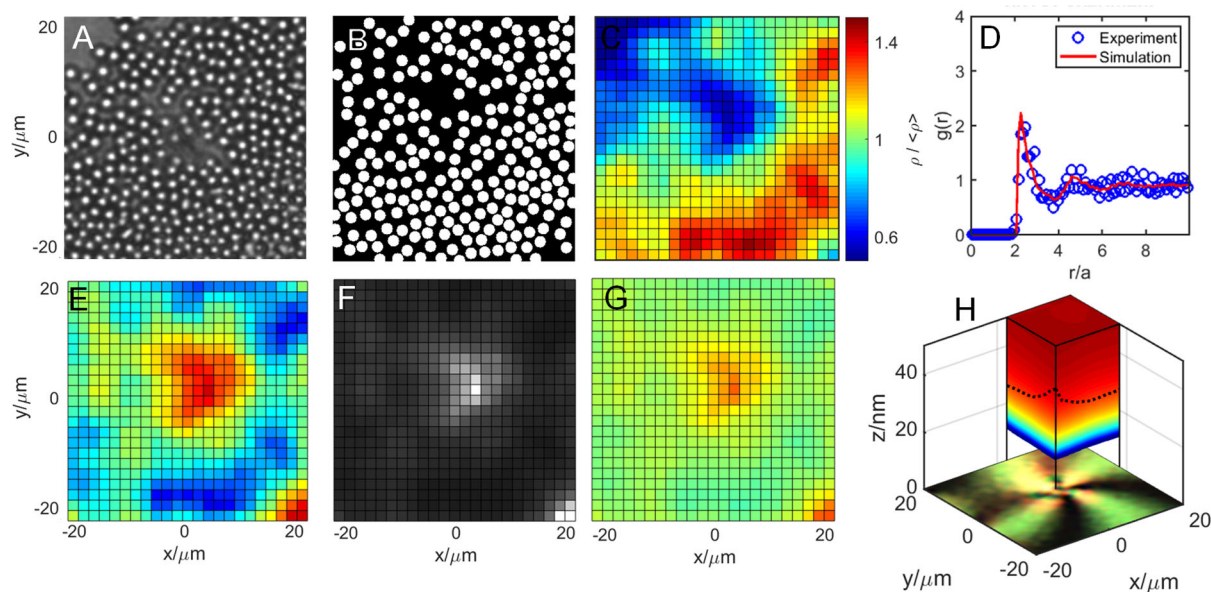


Fig. S3. Summary of diffusing colloidal probe experimental results, inverse MC simulations, and analysis of PLC defect in Fig. 5C. Representative configurations from (A) optical microscopy image of particles on PLC defect, and (B) rendering from converged equilibrated inverse MC simulation. (C) Experimental density profile over defect. (D) Pair correlation function from experiment (blue circles) and MC simulation (red line). (E) Converged interfacial energy landscape determined from inverse MC simulation ($u(x,y)=-6-0kT$, blue-red). (F) Position dependent brush thickness, ($2L_0(x,y)=25-35nm$, black-white). (G) van der Waals landscape evaluated at the onset of macromolecular repulsion ($u_v(x,y)=-4-0kT$, red-blue). (H) Optical characterization image and energy landscape quadrant cross sectional view centered on the defect with a dashed line showing the brush layer thickness at $h=2L_0$. Panels A-D are reported prior to removing the effect of surface tilt, whereas panel E-H show energy landscapes after removing the effect of a surface tilt (~ 350 nm over ~ 50 μm) on the gravitational contribution.